

## Hot and Warm Deformation of AA5182 Sheet Materials: Ductility and Microstructure Evolution

Eric M. Taleff<sup>1</sup>, Ken Takata<sup>2</sup> and Koji Ichitani<sup>3</sup>

<sup>1</sup>Department of Mechanical Engineering, The University of Texas at Austin, Austin, TX 78712-0292, U.S.A.

<sup>2</sup>Steel Research Laboratories, Nippon Steel Corporation, 20-1 Shintomi, Futtsu-city, Chiba, 293-8511, Japan.

<sup>3</sup>Furukawa-Sky Aluminum Corporation, 1352 Uwanodai, Fukaya-city, Saitama, 366-8511 Japan.

The 5000-series aluminum alloys, which contain magnesium as the primary alloying addition, exhibit remarkable ductilities and formabilities at elevated temperature. This makes possible the forming of very complex components from sheet materials. Superplastic forming has long used fine-grained AA5083 sheet to form such components, particularly for aerospace and transportation applications. However, new generations of hot-forming technologies are now utilizing lower temperatures, faster forming rates and less exotic materials to economically produce components of quite complex shape in large quantities. Among the materials suitable for these new processes, and future hot- and warm-forming processes not yet in commercial practice, is AA5182 sheet. We examine metallurgical reasons for the excellent formabilities exhibited by AA5182, including the influence of grain size, alloy content, deformation mechanisms and damage/failure mechanisms. In particular, we closely examine unique aspects of microstructural evolution in AA5182 which can strongly affect service properties, such as abnormal grain growth. In conclusion, we will consider the behavior of AA5182 in relation to a broad understanding of hot and warm deformation of aluminum-magnesium alloys.

**Keywords:** AA5182, hot forming, warm forming, superplasticity, abnormal grain growth

### 1. Introduction

The transportation industry is highly motivated to decrease vehicle mass in order to improve vehicle performance and efficiency. A reduction of mass reduces fuel consumption for vehicles powered by internal-combustion engines and increases driving range for electric vehicles. Aluminum alloys offer an effective and economical means of reducing the mass of vehicle body structures. However, utilization of aluminum alloys in vehicle structural components can be limited by the ability to form complex part shapes. Superplastic forming of aluminum alloys is a process used to produce parts with very complex shapes for the aerospace and niche automotive industries [1,2]. Superplastic forming requires specialized superplastic sheet materials and relatively long forming times. The automotive industry has recently adopted new hot-forming technologies to economically produce complex part shapes in aluminum alloy sheet for mass-production vehicles [3-6]. These hot-forming techniques utilize special grades of aluminum-magnesium alloys (i.e. 5000-series alloys), which achieve very high tensile ductilities at temperatures of 450 °C and higher. These technologies are a significant advance beyond classical superplastic forming technology because they use faster forming rates and lower temperatures. Material with a grain size coarser than is required for superplastic forming may also be used in some cases, which can produce significant cost savings. The potential to further advance these technologies toward forming at yet lower temperatures and faster rates with less expensive materials is not fully understood. Recent research results from aluminum-magnesium alloy AA5182 sheets for tensile ductility across a range of temperatures and strain rates [7] and for microstructural evolution during hot forming [8] provide new insight into this untapped potential. These results are reviewed and discussed.

## 2. Experimental Procedures

Two AA5182 alloy sheet materials are investigated, and both have initial recrystallized lineal-intercept grain sizes of approximately 14 to 17  $\mu\text{m}$ . These materials have as-received sheet thicknesses of 1.0 and 3.0 mm and compositions as listed in Table 1. The 1-mm sheet material was subjected to tensile tests at strain rates from  $10^{-3}$  to  $3 \times 10^{-2} \text{ s}^{-1}$  and temperatures from 100 to 400  $^{\circ}\text{C}$ . Tensile coupons had a gage length of 25 mm, a gage width of 6 mm and the same thickness of the as-received material. Temperature was controlled to within approximately  $\pm 1.5$   $^{\circ}\text{C}$  along the gage length during testing. Additional details of mechanical testing are described in Refs. [7,8]. Data obtained from these tests include flow stress at a true strain of  $\varepsilon = 0.2$ , strain-rate sensitivity and elongation to fracture. Selected specimens of the 3-mm sheet material were tested in tension, using the same specimen gage length and thickness, at a temperature of 400  $^{\circ}\text{C}$  and a strain rate of  $3 \times 10^{-2} \text{ s}^{-1}$ . The microstructures of these thicker specimens were examined after mechanical testing. Metallographic preparation included standard polishing and grinding techniques and then electrolytic etching at 25 V for approximately 60 s in Barker's reagent. Microstructures were observed in an optical microscope using polarizing filters. Details of metallographic examination procedures follow those described in Ref. [8].

Table 1: Composition of the AA5182 materials in wt. pct.

$t_0$ (mm)	Si	Fe	Cu	Mn	Mg	Cr	Zn	Ti	Al
1.0	0.09	0.22	0.03	0.35	4.44	0.03	0.01	0.02	Bal.
2.0	0.11	0.18	0.10	0.36	4.40	0.04	0.02	0.02	Bal.

## 3. Flow Behaviors and Tensile Ductility

Fig. 1 presents data from tensile tests of the 1-mm AA5182 material. Flow stress data were first normalized by the unrelaxed, temperature-dependent elastic modulus using the following fit to the data of Köster [9],

$$E = 77,630 - 12.98 T - 0.03084 T^2, \quad (1)$$

where  $E$  is in MPa and  $T$  is absolute temperature in K. In order to create the master curve for normalized flow stress, as shown in Fig. 1(a), data were collapsed onto a single curve by combining temperature and strain rate into the Zener-Hollomon parameter,

$$Z = \dot{\varepsilon} \exp\left(\frac{Q}{RT}\right), \quad (2)$$

where  $Q = 136$  kJ/mol is the activation energy for plastic flow, which is approximately that for magnesium diffusion in aluminum, and  $R$  is the universal gas constant.

The flow data of Fig. 1(a) can be described as falling into approximately three different flow regimes [7]. For  $Z < 10^{11} \text{ s}^{-1}$ , steady-steady creep occurs. In this regime, the strain-rate sensitivity, which is equal to the slope of the data in Fig. 1(a), is approximately  $m = 0.25$ . The flow stress quickly reaches a steady state, which does not vary significantly with strain, and deformation is well described by the theory of solute-drag creep [10,11]. The high strain-rate sensitivity in this regime produces high tensile ductilities. Strain-rate sensitivity is plotted against the logarithm of the Zener-Hollomon parameter in Fig. 1(b). Also indicated in Fig. 1(b) are the three deformation regimes observed from the data of Fig. 1(a). The second regime occurs for approximately  $10^{11} < Z$

$< 10^{16} \text{ s}^{-1}$ , and it is the power-law-breakdown (PLB) regime [12]. The PLB regime is characterized by dependence of flow stress on strain and can be considered as the transition from creep deformation into room-temperature flow behaviors. At the fastest strain rates and lowest temperatures,  $Z > 10^{16} \text{ s}^{-1}$ , the Portevin-Le Chatelier (PLC) effect becomes evident. This dynamic strain aging behavior occurs because of interaction between the magnesium solute atoms and dislocations. In the PLC regime, strain-rate sensitivity becomes negative. A negative strain-rate sensitivity is expected to produce very low tensile ductilities because of accelerated neck formation and growth.

Fig. 1(c) presents data for tensile elongation-to-fracture as a function of the logarithm of the Zener-Hollomon parameter. Tensile ductility generally follows the previously described effects from strain-rate sensitivity. The one important exception occurs for  $Z < 10^9 \text{ s}^{-1}$ . In this range, tensile elongation decreases with decreasing Zener-Hollomon parameter. This is not an effect of the strain-rate sensitivity, but is because of a change in failure mechanism. At larger values of  $Z$ , tensile ductility is generally limited by the formation of a pronounced neck, which is followed by ductile fracture. At small values of  $Z$ , significant microstructural damage can occur through cavity formation prior to extensive necking. Ductile fracture then results from cavity interlinkage with moderate to little neck formation. The value of  $Z$  at which maximum tensile ductility occurs is a result of this balance between neck growth and microstructural damage through cavitation. For the 1-mm AA5182 material, maximum tensile ductility occurs at approximately  $Z = 10^9 \text{ s}^{-1}$ , which is equivalent to a strain rate of  $0.03 \text{ s}^{-1}$  at  $400 \text{ }^\circ\text{C}$ .

#### 4. Microstructure Evolution and Abnormal Grains

Tensile ductility is not the only factor that determines the potential for usable ductility of aluminum materials in hot- and warm-forming operations. Microstructure evolution has been shown to be a critical factor limiting usable ductilities in hot-forming operations. Abnormal grains have been observed after hot forming of aluminum-magnesium alloys, and these large grains can reduce yield strength sufficiently to cause serious issues with part performance. Fig. 2 demonstrates several abnormal grains developed in the 3-mm AA5182 material following tensile deformation at  $400 \text{ }^\circ\text{C}$  and  $3 \times 10^{-2} \text{ s}^{-1}$ . These abnormal grains are the result of local strain-induced recrystallization [8]. Surprisingly, these abnormal grains do not form during hot deformation, but form only during annealing or slow cooling following hot deformation [8]. Hot deformation produces elongated grains containing many subgrains, as shown in Fig. 3. Grains are separated by high-angle boundaries, and subgrains are separated by low-angle boundaries. The formation of such a microstructure is related to the geometric dynamic recrystallization process [8,13,14]. Strains exceeding a critical strain, approximately  $\epsilon = 1.1$  for this material, produce nuclei which can recrystallize into the abnormal grains shown in Fig. 2. These nuclei are currently thought to be subgrains at the extreme ends of deformed grains, which contain a large fraction of high-angle boundary. Although plastic straining suppresses recrystallization, recrystallization can occur after the cessation of plastic flow. Strain beyond the critical strain increases the density of nuclei for recrystallization. Extended annealing then allows for recrystallization and growth of recrystallized grains to run to completion. This is demonstrated in Fig. 4, which presents the cross-section of a tensile coupon following extended annealing. As local strain increases into the heavily necked region, going from right to left, the average recrystallized grain size decreases. Fig. 5 presents experimental data for the areal density of recrystallized grains as a function of local true strain, calculated from local area reduction. The density of recrystallized grains is zero below the critical strain. As strain increases, recrystallized grain density increases, just as the density of nuclei for recrystallization increases. To avoid abnormal grains, the recrystallization process must be avoided. This can be accomplished by limiting strains to less than the critical strain.

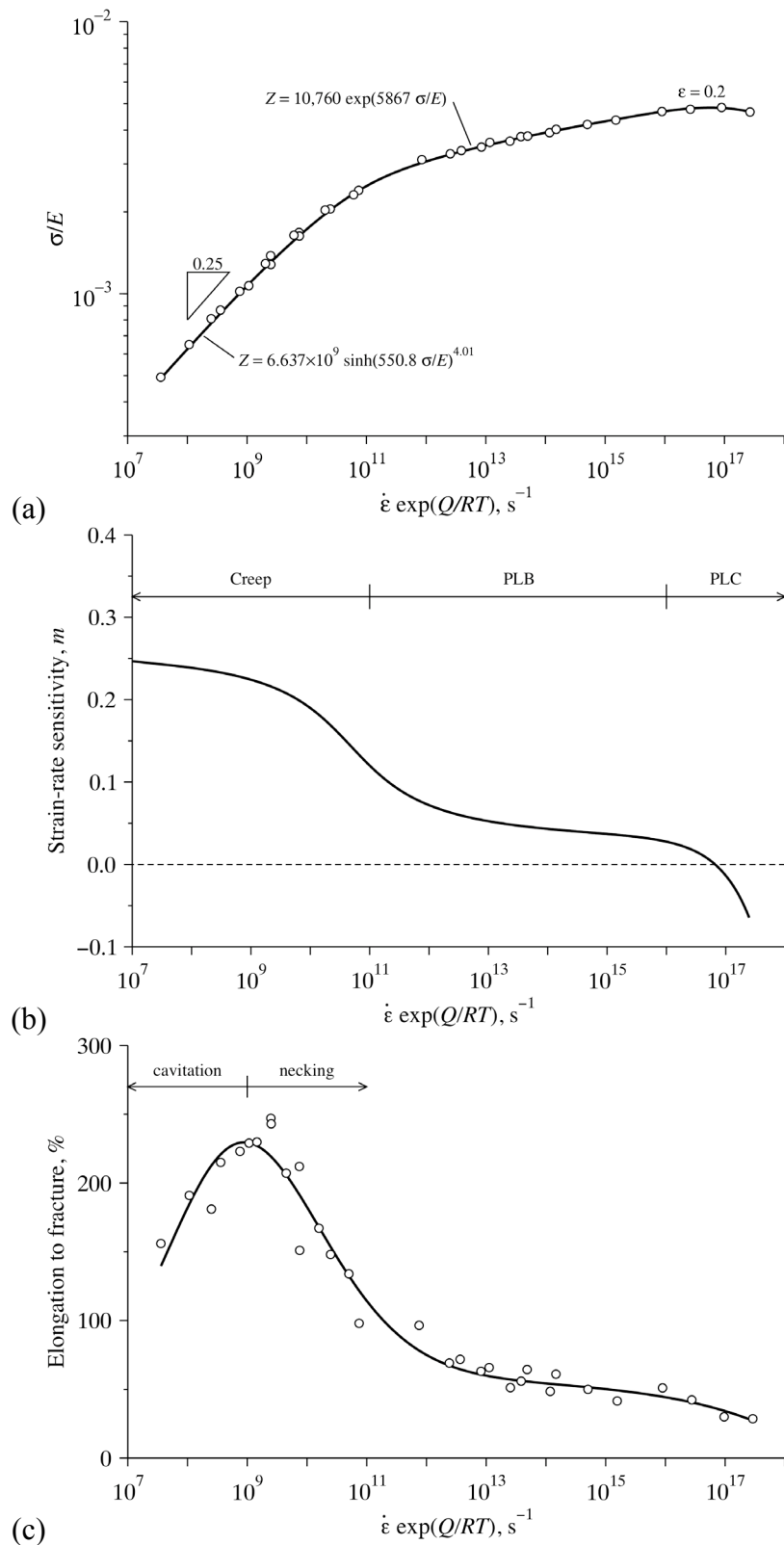


Figure 1: Data are shown from tensile tests of 1-mm AA5182 sheet material as a function of the Zener-Hollomon parameter, assuming  $Q = 136$  kJ/mole, for (a) modulus-compensated flow stress, (b) strain-rate sensitivity and (c) elongation to fracture.

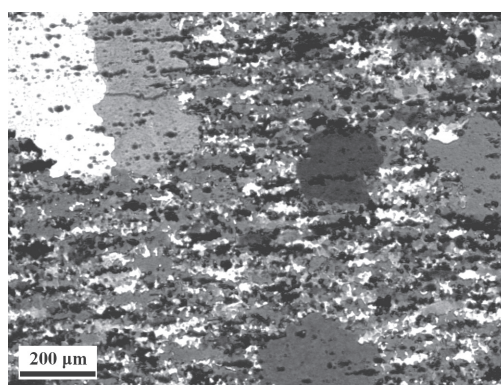


Figure 2: This photomicrograph of 3-mm AA5182 material following deformation at 400 °C and  $3 \times 10^{-2} \text{ s}^{-1}$  shows several abnormal grains developed during air cooling following deformation. The tensile axis is horizontal.

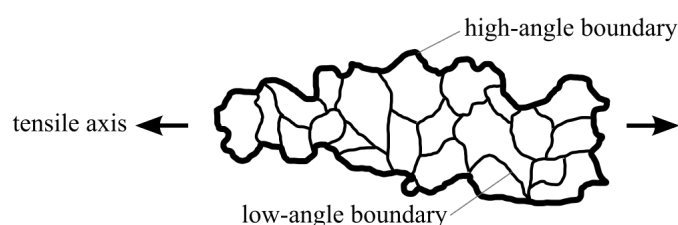


Figure 3: A schematic is shown of a deformed grain created by large tensile deformation of an aluminum-magnesium alloy.

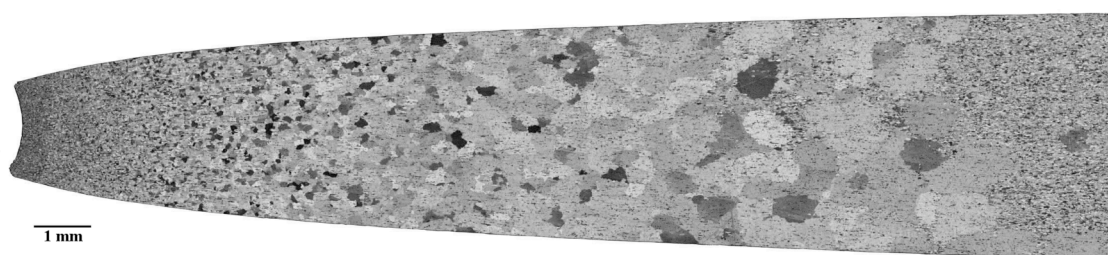


Figure 4: This composite photomicrograph of a tensile coupon demonstrates the effect of strain on recrystallization and abnormal grain formation in the 3-mm AA5182 material. The specimen was tested in tension at 400 °C and  $10^{-1} \text{ s}^{-1}$ , immediately water quenched and then annealed at 400 °C for 30 minutes. The tensile axis is horizontal.

## 5. Conclusions

The aluminum-magnesium alloy AA5182 can achieve excellent tensile ductilities across a range of hot- and warm-forming conditions. Usable ductilities for hot forming are limited by neck formation, cavitation damage and microstructural evolution leading to abnormal grains. Abnormal grains can be avoided by limiting forming strains to those less than the critical strain for recrystallization. Under warm-forming conditions, tensile ductility is generally limited by neck formation, which precedes ductile fracture. Very high usable tensile ductilities exist across a range of temperatures and strain rates not yet utilized in typical commercial forming techniques. New forming technologies which take advantage of these high ductilities are possible.

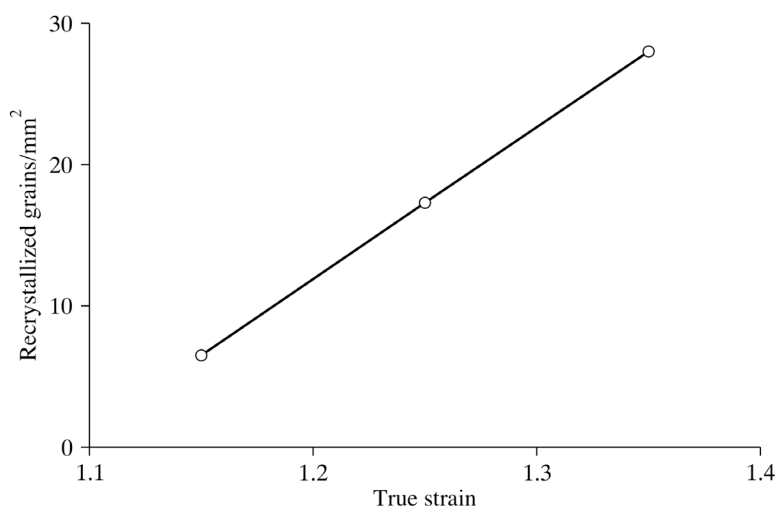


Figure 5: The areal density of recrystallized grains following tensile testing of 3-mm AA5182 at 400 °C and air cooling is shown as a function of local strain.

### Acknowledgements

The authors thank J.-K. Chung for the photomicrograph shown in Fig. 2 and A. J. Carpenter and J. P. Jodlowski for the composite photomicrograph shown in Fig. 4. E. M. Taleff gratefully acknowledges support for this work from the National Science Foundation (DMR-0605731).

### References

- [1] A.J. Barnes: *Materials Science Forum* 304-306 (1999) 785-796.
- [2] A.J. Barnes: *Materials Science Forum* 357-359 (2001) 3-16.
- [3] J. G. Schroth: *Advances in Superplasticity and Superplastic Forming*, Ed. By E. M. Taleff, P. A. Friedman, P. E. Krajewski, R. S. Mishra, and J. G. Schroth, (TMS, Warrendale, PA, 2004) pp. 9-20.
- [4] H. Kazama, K. Nakao, K. Takata, O. Noguchi, and Y. Suzuki: *Proceedings of the 108th Conference of the Japan Institute of Light Metals*, (Japan Institute of Light Metals, Tokyo, Japan, 2005) pp. 61-62.
- [5] F. Fukuchi, T. Yahaba, H. Akiyama, T. Ogawa, H. Iwasaki, and I. Hori: *Honda R&D Technical Review* 16 (2004) pp. 23-30.
- [6] K. Shiotsuki, H. Akiyama, I. Hori, K. Kashiwazaki, and S. Ueno: *Proceedings of the 107th Conference of the Japan Institute of Light Metals*, (Japan Institute of Light Metals, Tokyo, Japan, 2004) pp. 319-320.
- [7] J.-K. Chang, K. Takata, K. Ichitani and E. M. Taleff: *Mater. Sci. Eng. A* (2010) doi:10.1016/j.msea.2010.02.042
- [8] J.-K. Chang, K. Takata, K. Ichitani and E. M. Taleff: *Metall. Mater. Trans. A* (2010) accepted for publication.
- [9] W. Köster: *Z. Metallkunde* 29 (1948) pp. 1-9.
- [10] E. M. Taleff, P. J. Nevland and P. E. Krajewski: *Metall. Mater. Trans. A* 32A (2001) pp. 1119-1130.
- [11] J. Weertman: *Trans. Metall. Soc. AIME* 218 (1960) pp. 207-218.
- [12] O. D. Sherby and P. M. Burke: *Prog. Mater. Sci.* 13 (1968) pp. 325-390.
- [13] G. A. Henshall, M. E. Kassner, and H. J. McQueen: *Metall. Trans. A* 23A (1992) pp. 881-889.
- [14] H. J. McQueen: *Mater. Sci. Eng. A* 387-389 (2004) pp. 203-208.